

NL97F3977

STRUCTURAL AND THERMODYNAMIC CHARACTERIZATION OF THE PEROVSKITE-RELATED $\text{Ba}_{1+y}\text{UO}_{3+x}$ AND $(\text{Ba},\text{Sr})_{1+y}\text{UO}_{3+x}$ PHASES

E.H.P. CORDFUNKE
A.S. BOOIJ
V. SMIT-GROEN
P. VAN VLAANDEREN
D.J.W. IJDO

28 - 10

The Netherlands Energy Research Foundation ECN is the leading institute in the Netherlands for energy research. ECN carries out basic and applied research in the fields of nuclear energy, fossil fuels, renewable energy sources, policy studies, environmental aspects of energy supply and the development and application of new materials.

ECN employs more than 800 staff. Contracts are obtained from the government and from national and foreign organizations and industries.

ECN's research results are published in a number of report series, each series serving a different public, from contractors to the international scientific world.

This RX-series is used for publishing pre-prints or reprints of articles that will be or have been published in a journal, or in conference or symposium proceedings.

Please do not refer to this report but use the reference provided on the title page: 'Submitted for publication to ...' or 'Published in ...'.

Het Energieonderzoek Centrum Nederland (ECN) is het centrale instituut voor onderzoek op energiegebied in Nederland. ECN verricht fundamenteel en toegepast onderzoek op het gebied van kernenergie, fossiele-energiedragers, duurzame energie, beleidsstudies, milieuaspecten van de energievoorziening en de ontwikkeling en toepassing van nieuwe materialen.

Bij ECN zijn ruim 800 medewerkers werkzaam. De opdrachten worden verkregen van de overheid en van organisaties en industrieën uit binnen- en buitenland.

De resultaten van het ECN-onderzoek worden neergelegd in diverse rapportenseries, bestemd voor verschillende doelgroepen, van opdrachtgevers tot de internationale wetenschappelijke wereld.

Deze RX-serie wordt gebruikt voor het uitbrengen van pre-prints of reprints van artikelen die in een tijdschrift of in proceedings van conferenties of symposia (in definitieve vorm) zullen verschijnen of al zijn verschenen.

Gelieve niet te refereren aan het rapportnummer, maar de verwijzing te gebruiken die hiernaast op de titelpagina figureert: 'Voor publicatie aangeboden aan ...' of 'Verschenen in ...'.

Netherlands Energy Research Foundation ECN
P.O. Box 1
NL-1755 ZG Petten
the Netherlands
Telephone : +31 2246 49 49
Fax : +31 2246 44 80

This report is available on remittance of Dfl. 35 to:
ECN, Facility Services,
Petten, the Netherlands
Postbank account No. 3977703.
Please quote the report number.

© Netherlands Energy Research Foundation ECN

Energieonderzoek Centrum Nederland
Postbus 1
1755 ZG Petten
Telefoon : (02246) 49 49
Fax : (02246) 44 80

Dit rapport is te verkrijgen door het overmaken van f 35,- op girorekening 3977703 ten name van:
ECN, Faciliteiten
te Petten
onder vermelding van het rapportnummer.

© Energieonderzoek Centrum Nederland



KS002143281
R: FI
DE00971481X



DE00971481X

STRUCTURAL AND THERMODYNAMIC CHARACTERIZATION OF THE PEROVSKITE-RELATED $\text{Ba}_{1+y}\text{UO}_{3+x}$ AND $(\text{Ba},\text{Sr})_{1+y}\text{UO}_{3+x}$ PHASES

E.H.P. CORDFUNKE
A.S. BOOIJ
V. SMIT-GROEN
P. VAN VLAANDEREN
D.J.W. IJDO

Structural and thermodynamic characterization
of the perovskite-related $Ba_{1+y}UO_{3+x}$ and $(Ba, Sr)_{1+y}UO_{3+x}$ phases

E.H.P. Cordfunke, A. S. Booij, V. Smit-Groen, and P. van Vlaanderen
Netherlands Energy Research Foundation ECN,
P.O. Box 1, 1755 ZG Petten, The Netherlands

and

D.J.W. IJdo,
Gorlaeus Laboratories,
Leiden University,
P.O. Box 9502, 2300 RA Leiden, The Netherlands

Received

Abstract:

The perovskite-type $BaUO_3$ structure has been investigated by X-ray and neutron diffraction. The Ba/U ratio, the (Ba, Sr)/U ratio, and the oxygen stoichiometry in $Ba_{1+y}UO_{3+x}$ were varied, and the integral enthalpies of formation determined by solution calorimetry. In addition, equilibrium oxygen partial pressures were measured using a reversible EMF cell. The chemical defect mechanism is discussed, and it is shown that a continuous series $BaUO_3$ - $Ba_{1+y}UO_{3+x}$ - Ba_3UO_6 exist in which uranium vacancies are gradually filled up with barium ions, whereas uranium is oxidized via the pentavalent to the hexavalent state in Ba_3UO_6 (= $Ba_2(Ba,U)O_6$).

1. INTRODUCTION

Complex actinide oxides with one or more metal ions in addition to the actinide ions, are of interest because they can be formed during fission in nuclear fuel. Thus, the so-called "grey phase" is obtained as inclusions in highly irradiated UO_2 or $(\text{U,Pu})\text{O}_2$ fuel. This phase has the perovskite-type ABO_3 structure and contains, apart from the cations on the A sites (barium and strontium), on the B sites uranium and elements, such as plutonium and zirconium. Its general formula is $(\text{Ba,Sr,Cs})(\text{U,Pu,Zr,Mo,})\text{O}_3$ (1).

The fission products strontium and barium exhibit different behaviour in irradiated fuels. Whereas the oxide of strontium is predominantly dissolved in UO_2 , the majority of barium is precipitated in the grey phase (2,3). A knowledge of the chemical state of these fission products in irradiated fuels is of importance for an understanding of the fuel performance, and for their behaviour under accident circumstances. To this purpose a series of investigations was carried out in our laboratories to characterize the ABO_3 -type perovskites, with $\text{A} = \text{Ba}$ and Sr , and $\text{B} = \text{U}$. In a previous paper we reported a study of the perovskite-type strontium uranate (4). Instead of SrUO_3 a new phase with the formal composition $\text{Sr}_2\text{UO}_{4.5}$, was found with a statistical distribution of Sr and U^{5+} on one of the octahedral positions and one U^{5+} on the other position, leading to the formula $\text{Sr}_2(\text{Sr}_{2/3}\text{U}_{1/3})\text{UO}_6$. Ternary oxides ABO_3 ($\text{A} =$ alkaline earth metal and $\text{B} =$ actinide metal) have been studied by many authors (5-8), and the various aspects related with thermal stability and defect mechanisms have been discussed. In the present study the BaUO_3 structure was investigated in which both the Ba/U ratio and the oxygen stoichiometry were varied. In addition, partial replacement of barium by strontium was studied with the aim to clarify the difference in behaviour of barium and strontium in these perovskite-type structures.

2. EXPERIMENTAL

The starting materials for the preparation of BaUO_3 were BaO and UO_2 . The latter compound was prepared by reduction of U_3O_8 in hydrogen at 700°C , whereas BaO was prepared by decomposition of BaCO_3 (purified from strontium by recrystallization of the

starting material $\text{Ba}(\text{NO}_3)_2$, Baker p.a.) in a gold boat in high vacuum at 1000 °C. SrO was prepared by decomposition of SrCO_3 (Baker, p.a.) in high vacuum at temperatures which were gradually increased to 1050 °C. The alkaline earth uranates were prepared in X/U ratios ($X = \text{Ba}$ or $(\text{Ba} + \text{Sr})$) varying from 1.0 to 3.0, by heating the purified oxides in an (argon + hydrogen) atmosphere at a temperature of 950 °C, followed by heating the samples at temperatures of 1300 °C. Since the BaO in the samples reacts with both gold and platinum, it was necessary to heat them as pellets on already reacted pellets in crucibles of stabilized ZrO_2 . After the heatings the samples were stored in a glove box filled with dried argon.

The chemical analyses were carried out after dissolution of the sample in HCl and separation of the alkaline earths by an ion exchanger. Total U was determined titrimetrically with dichromate. In the case of only Ba the analysis of the alkaline earth was determined complexometrically with EDTA; in the case of two different alkaline earth metals the analyses were done with AES. All handlings of the samples, including the weighing, were carried out in an argon-filled, CO_2 -free dry glove box. The oxygen content of BaUO_{3+x} was determined from the weight increase by ignition of the sample in oxygen to BaUO_4 ; $\text{Ba}_{1+y}\text{UO}_{3+x}$ was determined from the analyzed Ba/U ratio, and the weight increase obtained by oxidizing the samples in oxygen at 1000°C to $\text{Ba}_3\text{UO}_6 + \text{BaUO}_4$.

Density measurements were done picnometrically with double-distilled CCl_4 . In order to achieve a satisfactory accuracy large samples (~ 5 g) were used in the determinations in a pycnometer with a contents of 25 cm³. In order to avoid trapped voids in the polycrystalline samples, the pycnometer was filled in vacuum; the measurements were done in triplo.

The X-ray diffraction patterns were made on single-coated film with a focusing Guinier camera (FR 552, Enraf Nonius, Delft, The Netherlands) using $\text{CuK}\alpha_1$ radiation ($\lambda = 1.5405981(3)$ Å) with $\alpha\text{-SiO}_2$ (hexagonal, $a = 4.9133(2)$, $c = 5.4053(4)$ Å) as an internal standard.

The neutron diffraction measurements were taken on the powder diffractometer at the HFR in Petten. Neutrons with $\lambda = 2.57176(3)$ Å were obtained using the beam reflected from

the hkl (111) planes of a single crystal of copper, reducing the λ/n contamination to less than 0.1% by means of a pyrolytic graphite filter. Soller slits with a horizontal divergence of 30' were placed between the reactor and the monochromator and in front of the four ^3He counters. The sample holder ($\varnothing = 1.43$ cm) consisted of a V tube closed with Cu plugs fitted with O-rings. The diffraction pattern was taken at 300 K and analysed by means of Rietveld's profile refinement technique (9). An absorption correction was applied according to Weber (10). For the coherent scattering lengths we used the values for O 5.805, Ba 5.07, Sr 7.02, and U 8.417 fm (11). For the refinement of the neutron diffraction data the program DBW 9006, version 8.491 was used (12). The variables include a scale factor, five background parameters, three half width parameters defining the Gaussian like peak shape, the counter zero, an asymmetry parameter, the unit cell dimensions, atomic position parameters and thermal parameters. A scale factor for the small contribution of the V sample holder was also refined. Three samples were studied by neutron diffraction, namely $\text{BaUO}_{3.05}$, $\text{Ba}_{1.553}\text{UO}_{3.866}$, and $(\text{Ba}_{0.92}\text{Sr}_{0.23})\text{UO}_{3.45}$.

The enthalpies of formation of BaUO_{3+x} and $\text{Ba}_{1+y}\text{UO}_{3+x}$ at 298.15 K were obtained from their enthalpies of solution in 0.77M HCl(+ FeCl_3) as measured in an isoperibol solution calorimeter at 298.15 K. The details of the calorimetric measurements have been described elsewhere (13).

The electromotive force (EMF) measurements were carried out, using a Keithley 617 electrometer, with a zirconia tube as the electrolyte, and separated electrode compartments. Temperature measurements were done with calibrated Pt/Pt, Rh(10%) thermocouples.

3. RESULTS

Synthesis of $\text{Ba}_{1+y}\text{UO}_{3+x}$

Attempts to prepare stoichiometric BaUO_{3+x} with a Ba/U ratio of 1.0 were unsuccessful. In all cases UO_2 was found as a secondary phase. A monophasic barium uranate was obtained at Ba/U ratios >1 , and it appeared that a solubility limit for barium in excess was obtained at Ba/U ratios >2.0 under the conditions of the synthesis (low oxygen pressures; see experimental). At higher ratios BaO was present as a secondary phase. As expected,

the volume of the unit cell increases with increasing Ba content till the solubility limit is reached. Fig. 1 shows the relationship between the volume of the pseudo-cubic "BaUO₃" cell and the Ba/U ratio. The results are given in Table 1 together with the O/U ratio of the samples.

Synthesis of (Ba, Sr)_{1+y}UO_{3+x}

In order to study the influence of the replacement of Ba by Sr ions on the BaUO₃-structure, samples containing (Ba + Sr)/U ratios up to 2.0 were prepared by heating mixtures of BaO, SrO and UO₂ under the same circumstances, as described for BaUO₃. It appeared to be possible to dissolve a little less than 1.0 mol SrO in the BaUO₃-structure, which resulted in a slight decrease of the cell volume (Fig. 1). At the ratio (Ba + Sr)/U = 2.0 some SrO was present as the second phase. As discussed in a previous paper (4), it is not possible to obtain SrUO₃, the compound Sr₂UO_{4.5} being formed instead. It appeared possible to dissolve BaO in this phase (Table 2); it is to be expected that the larger Ba ions will be situated on the A sites, where more space is available than on the B-sites.

Structure determinations

The structure of BaUO_{3.05} could be refined with space group Pbnm, analogous to BaPuO₃(14). The data given in Table 3, exhibit regular octahedra, as in BaPuO₃, which is, however, in disagreement with the earlier results of Barrett et al. (6). The latter authors assumed Ba vacancies to be present but from our neutron diffraction data it is not possible to discriminate between uranium and barium vacancies. The X-ray powder diffraction data of a second sample Ba_{1.553}UO_{3.866}(=Ba(Ba_{0.207} U_{0.777})O₃) indicate a nearly cubic, face-centered unit cell (a = 8.8 Å), but refinement of the neutron powder diffraction data with space group Fm3m, with U and (U + Ba) in octahedral positions, failed. Refinement in space group Pnma analogous to BaUO₃ also failed, but refinement in space group R $\bar{3}$ gave better results (Table 4). The simultaneous occupancy of one octahedral site by U and the other by (U + Ba), introduces a considerable disorder in the structure which cannot easily be modelled. As a consequence, only an average structure can be determined. A significant improvement was obtained when the statistic disorder was represented by anisotropic oxygen thermal parameters. It should be noted that the transition from a pseudo-cubic to a rhombohedral structure is only evident from the neutron diffraction work. The

structure of $(\text{Ba}_{0.92}\text{Sr}_{0.23})\text{UO}_{3.45}$ could be refined with space group Pbnm analogous to BaUO_{3+x} (Table 5). It has been assumed that in the compound, which can also be described as $(\text{B}_{0.84}\text{Sr}_{0.21})\text{U}_{0.87}\text{O}_3$, no vacancies are present in the A positions and in the O lattice; this is confirmed by density measurements, see Discussion.

The enthalpies of formation of $\text{Ba}_{1+y}\text{UO}_{3+x}$

The enthalpies of formation of five different barium uranate compositions were calculated from the enthalpy-of-solution data listed in Table 6, according to the reaction scheme given for one of the compositions, $\text{Ba}_{1.033}\text{UO}_{3.134}$, in Table 7. The reference data for the reactions 2 through 8 have been taken from recent publications by Cordfunke et al. (15,16). In Table 8 the enthalpies of formation of all samples are listed together with data for BaUO_4 and Ba_3UO_6 (17). A recent third-law evaluation of mass-spectrometric measurements of the dissociation pressures of $\text{BaUO}_{3.12}$, to give $\text{BaO}(\text{g})$ and $\text{UO}_2(\text{s})$ (18), yields for the enthalpy of formation $\Delta_f H^\circ(298.15\text{K}) = -1742.5 \pm 16.5 \text{ kJ}\cdot\text{mol}^{-1}$ in perfect agreement with the calorimetric results.

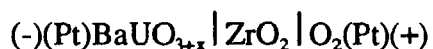
As expected, there is a linear correlation between the enthalpy of formation and the Ba/U ratio (Fig. 2), from which it is possible to extrapolate the enthalpy of formation of "BaUO₃" with a Ba/U ratio of 1.0 and x = 0:

$$\Delta_f H^\circ(298.15 \text{ K}) = -(1680 \pm 10) \text{ kJ}\cdot\text{mol}^{-1}$$

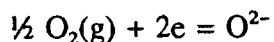
This value is in good agreement with previous determinations (5). This correlation is valid over the whole range from BaUO_3 , in which uranium has the formal valency of 4+, and Ba_3UO_6 , in which uranium is 6+.

The oxygen potential of BaUO_{3+x}

The thermodynamic stability of BaUO_{3+x} has been determined by measuring the oxygen potential of a reversible electromotive cell of the type:



in which ZrO_2 is a calcia-stabilized ZrO_2 tube which is closed at one side. The EMF cell has separated electrodes, with the reference electrode O_2 at a fixed pressure (air, $pO_2 = 0.2$ atm), and a sintered pellet of $Ba_{1+y}UO_{3+x}$ in an argon/CO(20%) atmosphere as the second electrode. Since the latter electrode is monophasic, the equilibrium



is a function of x in $Ba_{1+y}UO_{3+x}$ at a constant temperature. This can be measured either by coulometric titration or by analysis of the equilibrium composition at a certain temperature. Because the oxygen potential of $BaUO_{3+x}$ is very low near the stoichiometric composition, slight oxidation of the uranate via the gas phase always occurs, resulting in a slow drift of the EMF. For that reason we preferred to measure the EMF of the cell as a function of x in $BaUO_{3+x}$ at a fixed temperature. After each equilibrium measurement the composition was analyzed, as described before; the composition $Ba_{1.033}UO_{3.13}$ was taken as the starting material. When the equilibrium composition was reached, the cell was rapidly cooled down, and the composition determined by chemical analysis. It was assumed that during cooling the composition did not change. It was checked that the EMF's measured at a certain composition were reversible and reproducible. To that purpose a sample of $Ba_{1.033}UO_{3+x}$ was measured as a function of temperature up and down, and the composition determined after the measurements. The equilibrium was always attained rapidly. The results of the EMF measurements at three different temperatures are collected in Table 9 and shown in Fig. 3. For the two temperatures we obtain:

$$\text{at } 1060 \text{ K: } E(\text{mV}) = 1595.9 - 1138.2 \cdot x$$

$$1090 \text{ K: } E(\text{mV}) = 1494.6 - 874.8 \cdot x$$

The partial oxygen pressures for the various x -values calculated from these EMF values, are listed in Table 9.

DISCUSSION

Attempts to prepare stoichiometric $BaUO_{3.0}$ have always been unsuccessful; such

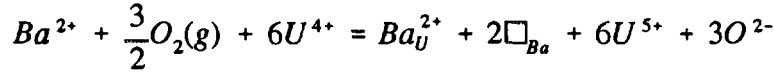
compositions always have a small amount UO_2 as a secondary phase. This has been found before (5,6), and is confirmed by the results of the present study. The equilibrium oxygen potential of stoichiometric $\text{BaUO}_{3.0}$ ($\sim -615 \text{ kJ}\cdot\text{mol}^{-1}$, see Table 9 and Fig. 2) is too low to be maintained during the preparation, and uptake of oxygen into the lattice will take place, either during the synthesis or during handling in the glove box. Thus, the phase $\text{BaUO}_{3.08}$ (Table 8) can be described as $\text{Ba}_{0.974}\text{U}_{0.974}\text{O}_3$, in which 2.6% of the uranium positions is empty, and having an equivalent number of Ba and U vacancies. By addition of BaO the vacancies are gradually filled up. In $\text{Ba}_{1.033}\text{UO}_{3.134}$ ($=\text{Ba}_{0.99}\text{U}_{0.957}\text{O}_3$) the uranium vacancies amount to 4.3%. In agreement herewith are the densities of $\text{BaUO}_{3.08}$ ($\text{Ba}_{0.974}\text{U}_{0.974}\text{O}_3$) and $\text{Ba}_{1.553}\text{UO}_{3.866}$ ($=\text{Ba}_{1.205}\text{U}_{0.776}\text{O}_3$) for which we calculate from the X-ray data the values 8.135 and $7.56^3\text{g}/\text{cm}^3$, respectively, which are to be compared with the experimentally determined values (8.08 ± 0.03) and (7.55 ± 0.03), respectively.

The perovskite-type barium uranate " BaUO_3 ", and its solid solutions with strontium differ considerably from the perovskite-type strontium uranate. In the latter case, the " SrUO_3 " phase was shown to be not stable (4), and stabilization of the uranate is only possible in the presence of oxygen by oxidation of U^{4+} to U^{5+} via defect chemical reactions to give a phase with the discrete composition $\text{Sr}_2(\text{Sr}_{2/3}\text{U}_{1/3})\text{UO}_6$ (or $\text{Sr}_2\text{UO}_{4.5}$), which is structurally related to Sr_3UO_6 ($=\text{Sr}_2(\text{Sr})\text{UO}_6$) (19), however, with only $2/3$ Sr per unit cell on a B site. At the same time a slight tilting of the UO_6 octahedra occurs which reduces the size of cavity which is occupied by the alkaline-earth metal ions. The tilting causes an orthorhombic distortion of the cubic perovskite structure.

Whereas the $\text{Sr}_2\text{UO}_{4.5}$ -phase has a discrete composition, the situation in " BaUO_3 " is totally different. Again, stabilization of BaUO_3 occurs by oxidation of U^{4+} ions via the formation of metal vacancies rather than oxygen interstitials, but now Ba is *gradually* placed in the U vacancies on the B site. In the Kröger-Vink notation:

$$\begin{aligned}
BaUO_3 + \frac{x}{2}O_2 &= Ba_{1-y}\square''_{\frac{x}{3+y}}(U_{1-2x}^x U_{2x}^{\circ} Ba_y'' \square'''_{\frac{x}{3-y}})O_{3+x} \\
&= \frac{3+x}{3} \left[Ba_{\frac{3-3y}{3+x}}^x \square_{\frac{x+3y}{3+x}} \left(U_{\frac{3-6x}{3+x}}^x U_{\frac{6x}{3+x}}^{\circ} Ba_{\frac{3y}{3+x}}'' \square_{\frac{x-3y}{3+x}}''' \right) O_3 \right]
\end{aligned}$$

or:



Although other defect mechanisms are possible, our neutron diffraction analysis and those by Barrett et al. (6), as well as lattice minimization calculations by Ball (20) suggest that the defect chemistry is dominated by anti-site disorder, and that the process of moving a lattice A ion into uranium vacancies is energetically favourable.

From the experiments listed in Table 1 it follows that BaUO₃ is able to take BaO into solid solution up to a maximum composition of approximately Ba/U > 2.0. As shown in Fig. 1 the volume of the unit cell gradually increases with the BaO content till the maximum solubility is reached. Then BaO is present as the secondary phase, and no indications for the oxide Ba₃UO₅, as suggested by Charvillat et al. (7), have been found. The saturation concentration of BaO in the BaUO₃ structure depends on the oxygen pressure which governs the uranium vacancies. Finally, with increasing oxygen potential e.g. in a H₂O/H₂ atmosphere, the pentavalent uranate Ba₂U₂O₇ will be formed, in agreement with observations by Braun et al. (8).

The solution of BaO into BaUO₃ can occur either substitutionally or interstitially with charge compensation through either vacancy or interstitials, and a variety of defect schemes can be formulated. Again, lattice minimization calculations clearly show that the preferred method of solution involves the substitution of Ba into the barium and uranium sites in the BaUO₃ structure (20), with charge compensation through anion vacancies (half an oxygen vacancy per AO formula unit dissolved), ultimately resulting in a phase of composition Ba₂(Ba,U)O₆. Stabilization of the BaUO₃-phase thus occurs via oxidation of U⁴⁺ to U⁵⁺, the creation of vacancies on the U-sites in the lattice, and the simultaneous placement of Ba-

ions in the U-vacancies, which ultimately leads to the Ba_3UO_6 structure ($= Ba_2(Ba,U)O_6$), in which U is in the hexavalent state, or Ba_2SrUO_6 (1). The system $Ba_2(Ba_xU_{1-x})UO_6$ is analogous to the system $Ba_2(Ba_xBi_{1-x})BiO_6$ (22). The end number $x = 0$ ($Ba_2Bi(III)Bi(V)O_6$) has a monoclinic structure at room temperature but above > 405 K it transforms to a rhombohedral structure. When additional barium atoms are introduced into the structure substitution of Ba for Bi(III) occurs to give a rhombohedral structure.

It is interesting to note that SrO also dissolves in the " $BaUO_3$ " structure, however, with a small decrease in the cell volume (Fig. 1 and Table 2), which follows from the ion sizes in the 12 coordination [Ba^{2+} 1.75 Å, Sr^{2+} 1.44 Å] compared with U^{5+} (0.76 Å) (23). Again, its solubility depends on the oxygen potential.

When the enthalpies of formation at 298.15 K of $Ba_{1+y}UO_{3+x}$ (Table 8) are plotted as a function of y , a linear relationship is obtained (Fig. 2). As expected, $\Delta_f H^\circ(Ba_3UO_6)$ is a point on this line, being a member of the perovskite-series $BaUO_3 - Ba_{1+y}UO_{3+x} - Ba_3UO_6$. In contrast, $Ba_2U_2O_7$, in which U is pentavalent, is not a member of this series, having a different crystal structure (24).

REFERENCES

1. H. Kleykamp, J.O. Paschoal, R. Pesja, and F. Thümmeler, *J. Nucl. Mat.* **130**, 426 (1985).
2. H. Kleykamp, *J. Nucl. Mat.* **131**, 221 (1985).
3. H. Kleykamp, *J. Nucl. Mat.* **206**, 82 (1993).
4. E.H.P. Cordfunke and D.J.W. IJdo, *J. Solid State Chem.* **109**, 272 (1994).
5. C.W. Williams, L.R. Morss, and In-Kyu Choi, *ACS Symposium Series*, no. **246** (1984), p. 323.
6. S.A. Barrett, A.J. Jacobson, B.C. Tofield, and B.E.F. Fender, *Acta Crystallogr.* **B38**, 2775 (1982).
7. J.P. Charvillat, G. Baud, and J.P. Besse, *Mat. Res. Bull.* **5**, 933 (1970).
8. R. Braun, S. Kemmler-Sack, H. Roller, I. Seemann, and I. Wall, *Z. anorg. allg. Chem.* **415**, 133 (1975).
9. H.M. Rietveld, *J. Appl. Crystallogr.* **2**, 65 (1969).
10. K. Weber, *Acta Crystallogr.* **23**, 720 (1967).
11. F. Sears, *Neutron News* **3**, 26 (1992).
12. D.B. Wiles and R.A. Young, *J. Appl. Crystallogr.* **14**, 149 (1981).
13. E.H.P. Cordfunke, W. Ouweltjes, and G. Prins, *J. Chem. Thermodynamics* **7**, 1137 (1975).
14. G.G. Cristoph, A.C. Larson, P.G. Eller, J.D. Purson, J.D. Zahrt, R.A. Penneman, G.H. Rinnehart, *Acta Crystallogr.* **B44**, 575-580 (1988).
15. E.H.P. Cordfunke and W. Ouweltjes, *J. Chem. Thermodynamics* **20**, 235-238 (1988).
16. E.H.P. Cordfunke, R.J.M. Konings, and W. Ouweltjes, *J. Chem. Thermodynamics* **22**, 991 (1990).
17. *Thermochemical Data for Reactor Materials and Fission Products*, E.H.P. Cordfunke and R.J.M. Konings (eds), Amsterdam (1990), p. 72-73.
18. M. Yamawaki, J. Huang, K. Yamaguchi, M. Yasumoto, H. Sakurai, and Y. Susuki, *J. Nucl. Mat.* **231**, 199-203 (1996).
19. D.J.W. IJdo, *Acta Crystallogr. Sect. C* **49**, 650 (1993).
20. R. G.J. Ball, *J. Mater. Chem.* **2**, 641 (1992).

21. W.A. Groen and D.J.W. IJdo, *Acta Cryst. C* **43**, 1033-1036 (1987).
22. K.P. Reis, A.J. Jacobson, and J.M. Nichol, *J. Solid State Comm.* **107**, 428-443 (1993).
23. R.D. Shannon, *Acta Cryst. A* **32**, 751 (1976).
24. E.H.P. Cordfunke and D.J.W. IJdo, *J. Phys. Chem. Solids* **49**, 551-554 (1988).

Table 1. Oxygen contents and cell volume of $Ba_{1+y}UO_{3+x}$ phases

y (Ba/U ratio)	x	phases (P=perovskite)	cell volume (\AA^3)*
1.033	3.135–3.133	P	685.0
1.038		P	685.3
1.040		P + tr.UO ₂	
1.065	3.163–3.181	P	686.9
1.086		P	685.8
1.182		P	689.5
1.238	3.417–3.397	P	693.1
1.371		P	694.6
1.400	3.595–3.613	P	697.4
1.499		P	697.8
1.553	3.864–3.867	P	699.6
1.631		P	700.5
1.766		P	701.9
1.809		P	703.1
2.140		P	706.3
2.635		P + BaO	706.9

* cell volume calculated with a cubic cell with $2a_0$, obtained from the Guinier measurements

Table 2. (Ba, Sr)UO_{3+x} compositions and cell volume of equilibrium phases

Sample	phase	cell volume (Å ³)
BaSr _{0.25} UO _{3+x}	BaUO ₃	682.1
BaSr _{0.50} UO _{3+x}	BaUO ₃	680.9
BaSr _{0.75} UO _{3+x}	BaUO ₃	677.9
BaSr _{1.00} UO _{3+x}	BaUO ₃ + SrO	677.4
Sr ₂ (Sr _{0.67} U _{0.33})UO ₆	Sr ₂ UO _{4.5}	640.7
Sr _{1.50} Ba _{0.5} (Sr _{0.5} U _{0.4} □ _{0.1})UO ₆	Sr ₂ UO _{4.5}	653.7
Sr _{1.33} Ba _{0.67} (Sr _{0.67} U _{0.33})UO ₆	Sr ₂ UO _{4.5} + SrO	657.9

Table 3. Fractional atomic coordinates and isotropic thermal parameters of $\text{Ba}_{0.99}\text{U}_{0.99}\text{O}_3$ (Pbnm)

	x	y	z	B(\AA^2)	occupation
Ba	0.9975(14)	0.0224(10)	0.25	1.25(10)	0.988(6)
U	0	0.5	0	0.25(5)	0.989(5)
O(1)	0.0699(10)	0.4966(12)	0.25	0.92(15)	1.0
O(2)	0.7266(9)	0.2735(9)	0.0389(5)	1.93(11)	1.0

$$a = 6.2590(7), \quad b = 6.2397(5), \quad c = 8.8123(8)\text{\AA}, \quad V = 344.16(6)\text{\AA}^3$$

$$\rho_{\text{calc}} = 8.087 \text{ g/cm}^3$$

$$R_p = 3.37, \quad R_{\text{wp}} = 4.57, \quad S = 1.71, \quad D -wD = 0.91$$

Table 3a. Atomic distances (\AA) and angles ($^\circ$) in $\text{Ba}_{0.99}\text{U}_{0.99}\text{O}_3$ at room temperature

Ba-O(1)	2.712(11)	4-O(1)	2.246(1)
Ba-O(1)	2.993(10)	-O(2)	2.245(6)
Ba-O(1)	3.312(10)	-O(2)	2.246(6)
Ba-O(2)	2.800(8) 2x	O(1)-U-O(2)	90.4(2)
	2.965(8) 2x	O(1)-U-O(2)	91.1(2)
	3.187(7) 2x	O(2)-U-O(2)	91.5(2)
		U-O(1)-U	157.5(3)
		U-O(2)-U	159.5(2)

Table 4. Refined profile and structural parameters for Ba₂(Ba_{0.414}U_{0.55})UO₆

atom	site	x	y	z	occupation	B(Å ²)
Ba(1)	2c	0.2455(22)	x	x	1.0	
U(1)	1a	0	0	0	1.0	
Ba(2)	1b	0.5	0.5	0.5		
U(2)	1b	0.5	0.5	0.5		
O(1)	6f	-0.2431(29)	0.1969	0.2934(29)	1.0	

$$a = 6.2711(6)\text{Å} \quad \alpha = 60.173(8) \quad R\bar{3}$$

$$R_p = 4.44 \quad R_{wp} = 5.60 \quad S = 3.56 \quad D -wD = 0.24$$

$$\rho_{\text{calc}} = 7.563 \text{ g/cm}^3 \quad \rho_{\text{exp}} = 7.55 \text{ g/cm}^3$$

Table 4a. Atomic distances (Å) and angles (°) in Ba₂(Ba_{1.44}U_{1.554})O₆ at room temperature

Ba-O(1)	2.806(16) 3x	U-O(1)	2.150(18) 6x
-O	3.127(28) 3x	Ba(2)/U(2)-O(1)	2.343(18) 6x
-O	3.183(28) 3x		

Table 5. Fractional atomic coordinates and isotropic thermal parameters of $\text{Ba}_{0.92}\text{Sr}_{0.08}(\text{Sr}_{0.13}\text{U}_{0.87})\text{O}_3$ (Pbnm)

	x	y	z	B(Å ²)
Ba/Sr	0.09968(24)	0.0248(3)	0.25	1.30(10)
U/Sr	0	0.5	0	0.65(6)
O(1)	0.0753(19)	0.4897(18)	0.25	2.50(6)
O(2)	0.7242(16)	0.2747(17)	0.0370(7)	2.50(6)

$$a = 6.2344(11), \quad b = 6.2245(8), \quad c = 8.7949(13)\text{Å}, \quad V = 341.30(11) \text{Å}^3$$

$$\rho_{\text{calc}} = 7.780 \text{ g/cm}^3; \quad \rho_{\text{exp}} = 7.77 \text{ g/cm}^3$$

$$R_p = 3.87 \quad R_{wp} = 5.00 \quad S = 1.92 \quad D - wD = 0.77$$

Table 5a. Atomic distances (Å) and angles (°) in $\text{Ba}_{0.92}\text{Sr}_{0.08}(\text{Sr}_{0.13}\text{U}_{0.87})\text{O}_3$ at room temperature.

Ba/Sr-O(1)	2.677(19)	U-O(1)	2.249(3)
-O(1)	2.935(14)	-O(2)	2.232(9)
-O(1)	3.367(14)	-O(2)	2.243(9)
-O(2)	2.798(12) 2x	O(1)-U-O(2)	90.6(33)
-O(2)	2.969(12) 2x	O(1)-U-O(2)	90.0(33)
-O(2)	3.153(18) 2x	O(2)-U-O(2)	91.3(32)
		U-O(1)-U	155.7(6)
		U-O(2)-U	159.7(4)

table 6. The molar enthalpy of solution of a mass m of $Ba_{1+y}UO_{3+x}$ in 250 cm^3 ($HCl + 0.0400FeCl_3 + 70.68H_2O$) at 298.15 K .

m/g	$\epsilon\Theta/J$	$\Delta\Theta/\theta$	$\Delta_{sol}H_m/kJ\cdot mol^{-1}$	Ba/U ratio	
a. $Ba_{1.033}UO_{3.134}$					
0.10635	120.5281	0.5426	-264.441		
0.10390	118.7923	0.5372	-264.124		
0.10497	119.7415	0.5409	-265.335		
			mean: -264.63 \pm 0.73		
b. $Ba_{1.065}UO_{3.172}$					
0.11443	119.4770	0.6156	-279.618		
0.11512	122.4086	0.6076	-281.061		
0.10784	120.7086	0.5752	-280.091		
			mean: -280.26 \pm 0.85		
c. $Ba_{1.238}UO_{3.407}$					
0.10541	120.4779	0.5656	-299.015		
0.10572	119.8305	0.5733	-300.573		
0.10398	118.9405	0.5627	-297.725		
			mean: -299.10 \pm 1.65		
d. $Ba_{1.400}UO_{3.604}$					
0.10780	119.4450	0.5985	-323.584		
0.10486	118.7794	0.5896	-325.884		
0.10364	120.6702	0.5707	-324.231		
			mean: -324.57 \pm 1.37		
e. $Ba_{1.553}UO_{3.866}$					
0.10573	120.1681	0.5751	-335.412		
0.10356	119.9638	0.5659	-336.390		
0.10594	119.6386	0.5778	-334.838		
			mean: -335.55 \pm 0.91		
f. $BaCl_2$ UCl_4					
0.05168	0.08982	119.6323	0.3911	-197.863	1.0495
0.06473	0.07431	120.2788	0.3309	-203.441	1.5890
0.04337	0.09512	117.3773	0.4177	-195.784	0.8317
0.07101	0.06791	118.3587	0.3119	-206.482	1.9074
0.06871	0.07404	119.2078	0.3339	-204.200	1.6928
0.08342	0.06108	120.5713	0.2841	-213.018	2.4913
0.05269	0.07607	121.0748	0.3317	-200.533	1.2635
0.05261	0.06294	117.6739	0.2872	-203.957	1.5247
0.08435	0.06665	117.3116	0.3146	-210.329	2.3085

Table 7. Reaction scheme for the standard molar enthalpy of formation of $\text{Ba}_{1.033}\text{UO}_{3.134}(\text{s})$ at the temperature 298.15 K.

$$\Delta H_9 = -\Delta H_1 + \Delta H_2 + \Delta H_3 + \Delta H_4 + \Delta H_5 + \Delta H_6 - \Delta H_7 + \Delta H_8$$

(sln) refers to $(\text{HCl} + 0.040\text{FeCl}_3 + 70.68 \text{H}_2\text{O})$

Reaction	$\Delta_{\text{sol}}H_{\text{m}}^{\circ}(\text{kJ}\cdot\text{mol}^{-1})$	
1. $\text{Ba}_{1.033}\text{UO}_{3.134}(\text{s}) + (2.268\text{HCl} + 1.798\text{FeCl}_3)(\text{sln})$	$= (1.033\text{BaCl}_2 + \text{UO}_2\text{Cl}_2 + 1.798\text{FeCl}_2 + 1.134\text{H}_2\text{O})(\text{sln})$	-264.63 ± 0.73
2. $1.033\text{BaCl}_2(\text{s}) + 0.899\text{UCl}_4(\text{s}) + (1.798 \text{FeCl}_3 + 1.798\text{H}_2\text{O})(\text{sln})$	$= (1.033\text{BaCl}_2 + 0.899\text{UO}_2\text{Cl}_2 + 1.798\text{FeCl}_2 + 3.596\text{HCl})(\text{sln})$	-199.13 ± 0.24
3. $0.101\text{UO}_2\text{Cl}_2(\text{s}) + \text{sln}$	$= 0.101\text{UO}_2\text{Cl}_2(\text{sln})$	-10.32 ± 0.06
4. $1.033\text{Ba}(\text{s}) + 1.033\text{Cl}_2(\text{g})$	$= 1.033\text{BaCl}_2(\text{s})$	-883.37 ± 1.79
5. $0.101\text{U}(\text{s}) + 0.101\text{O}_2(\text{g}) + 0.101\text{Cl}_2(\text{g})$	$= 0.101\text{UO}_2\text{Cl}_2(\text{s})$	-125.59 ± 0.13
6. $0.899\text{U}(\text{s}) + 1.798\text{Cl}_2(\text{g})$	$= 0.899\text{UCl}_4(\text{s})$	-915.90 ± 2.25
7. $2.932\text{H}_2(\text{g}) + 2.932\text{Cl}_2(\text{g}) + \text{sln}$	$= 5.864\text{HCl}(\text{sln})$	-966.33 ± 0.53
8. $2.932\text{H}_2(\text{g}) + 1.466\text{O}_2(\text{g}) + \text{sln}$	$= 2.932\text{H}_2\text{O}(\text{sln})$	-838.09 ± 0.12
9. $1.033\text{Ba}(\text{s}) + \text{U}(\text{s}) + 1.567\text{O}_2(\text{g})$	$= \text{Ba}_{1.033}\text{UO}_{3.134}(\text{s})$	-1741.44 ± 3.03

Table 8. The enthalpies of formation at 298.15 K of barium uranates

compound	molar ratio U ⁵⁺ /U	$\Delta_f H^\circ(298.15 \text{ K})$ /kJ·mol ⁻¹	ref.
BaUO _{3.05}	0.10	-1700.4 ± 3.1	
BaUO _{3.08}	0.16	-1710.0 ± 3.0	
Ba _{1.033} UO _{3.134}	0.20	-1741.4	
Ba _{1.065} UO _{3.172}	0.21	-1754.4	
Ba _{1.238} UO _{3.407}	0.34	-1902.0	
Ba _{1.400} UO _{3.604}	0.41	-2023.6	
Ba _{1.553} UO _{3.866}	0.63	-2182.2	
Ba ₂ U ₂ O ₇	1.0	-3739.8	15
Ba ₃ UO ₆	-	-3210.7	17

Table 9. EMF measurements vs composition for $\text{Ba}_{1.033}\text{UO}_{3.13}$

Temperature, K	composition, x in $\text{Ba}_{1.033}\text{UO}_{3+x}$	EMF, mV	$\log p\text{O}_2(\text{atm})$
1060	0.154	1407.0	-27.44
1060	0.204	1368.3	-26.73
1060	0.228	1346.8	-26.32
1060	0.265	1304.7	-25.53
1060	0.335	1202.6	-23.59
1084	0.238	1293.5	-24.76
1090	0.145	1371.1	-26.1
1090	0.185	1327.6	-25.3
1090	0.261	1268.0	-24.1

Figure Legends

1. The unit cell volume of $\text{Ba}_{1+y}\text{UO}_{3+x}$ and $(\text{Ba}, \text{Sr})_{1+y}\text{UO}_{3+x}$ as a function of the Ba/U ratio (\bullet) or the (Ba, Sr)/U ratio (\blacktriangle).
2. Observed (dots) and calculated (full line) neutron diffraction profiles of (a) $\text{BaUO}_{3.05}$, and (b) $(\text{Ba}_{0.92}\text{Sr}_{0.23})\text{UO}_{3.45}$ [$=\text{Ba}_2(\text{Ba}_{0.414}, \text{U}_{0.55})\text{UO}_6$].
Thick marks below the profiles indicate the positions of the Bragg reflections. Difference (observed-calculated) curves appear at the bottom of the plots. Two theta in degrees.
3. Variation of emf with x in $\text{Ba}_{1.033}\text{UO}_{3+x}$ at two different temperatures.
4. The relationship between enthalpy of formation and the Ba/U ratio in $\text{Ba}_{1+y}\text{UO}_{3+x}$ at 298.15 K.

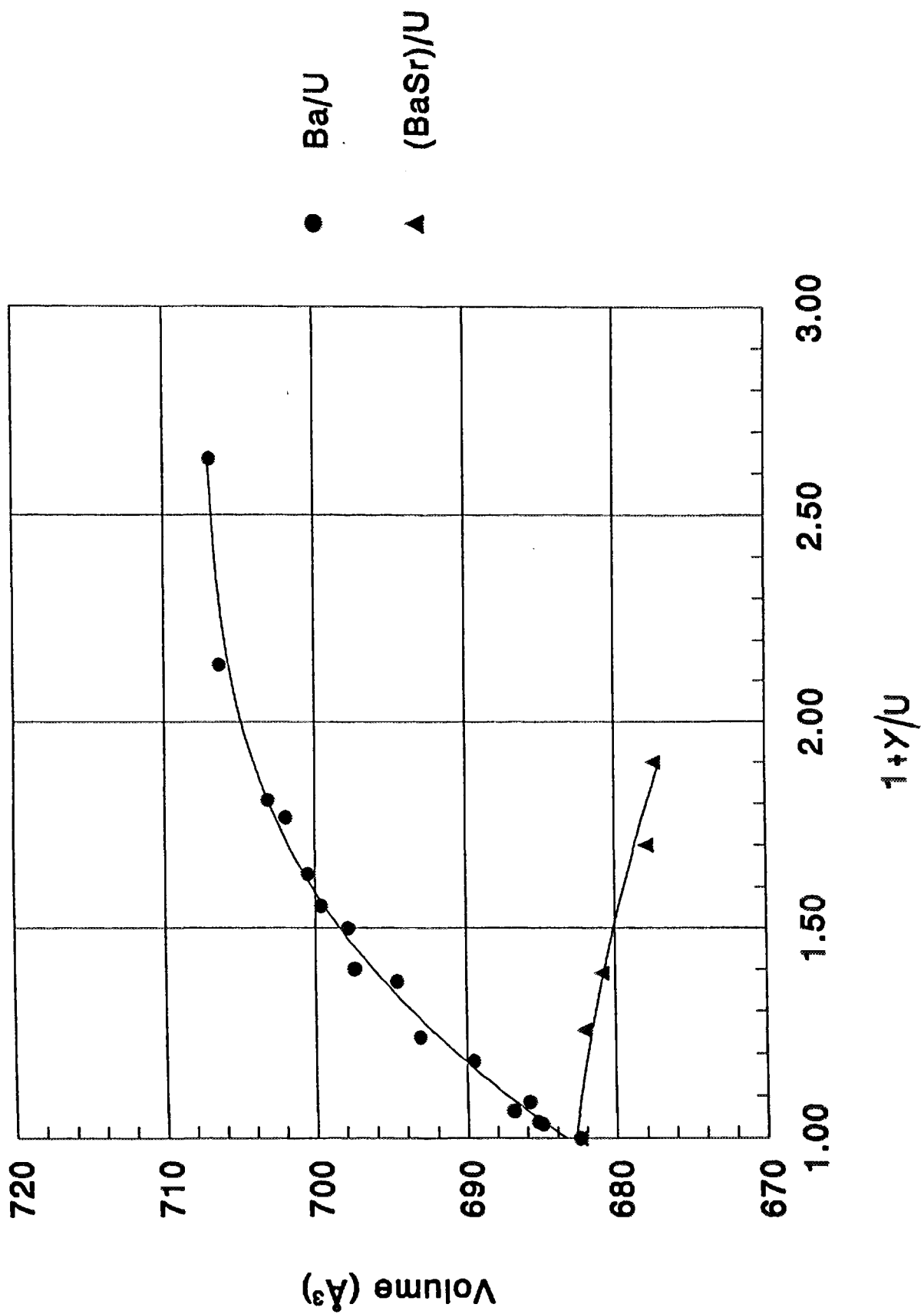
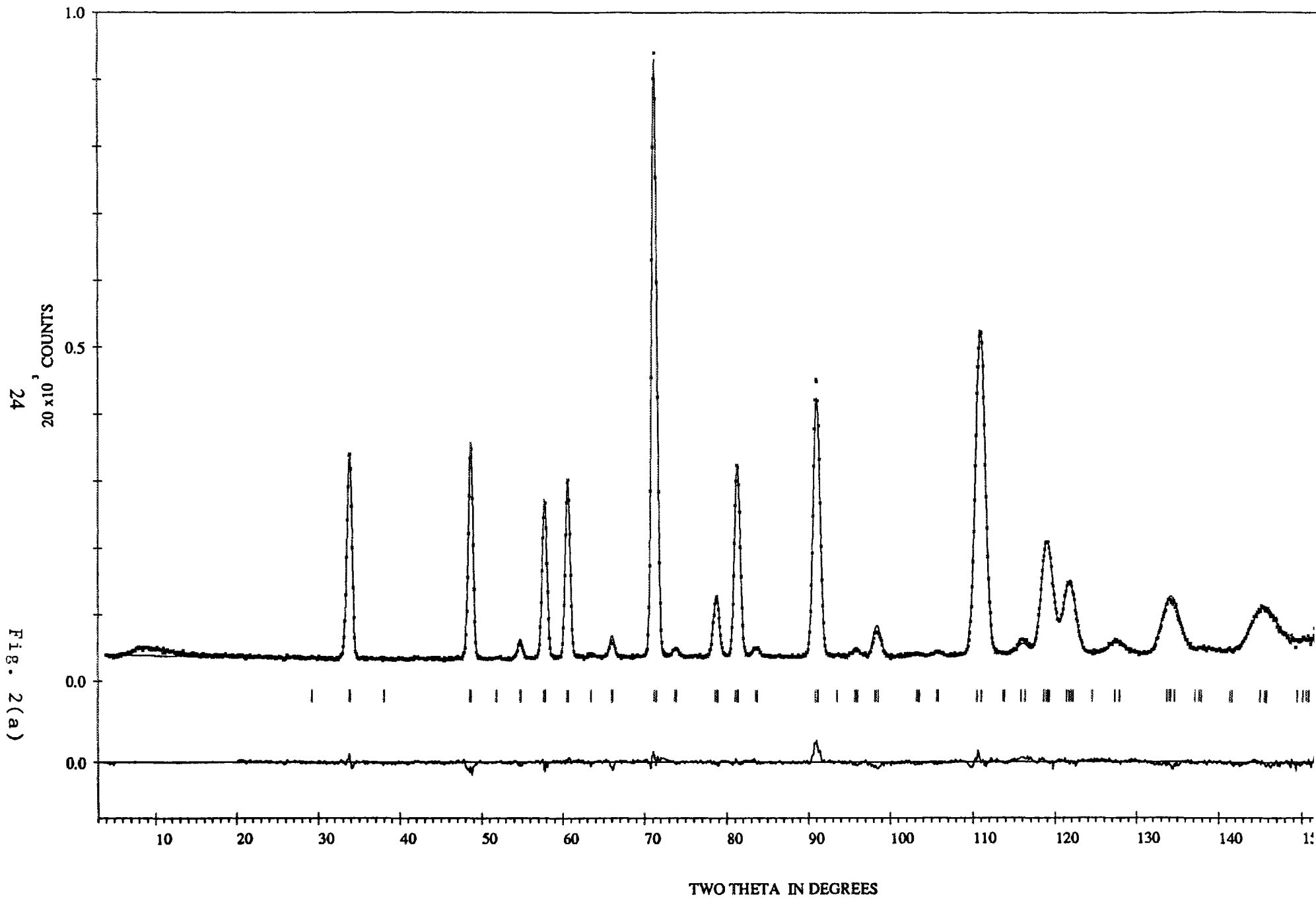


Fig. 1

BAUO3 1991 BA.99UO3 REFINED P N M A



BA.92SR.08U.87SR.1303 1991 PBNM

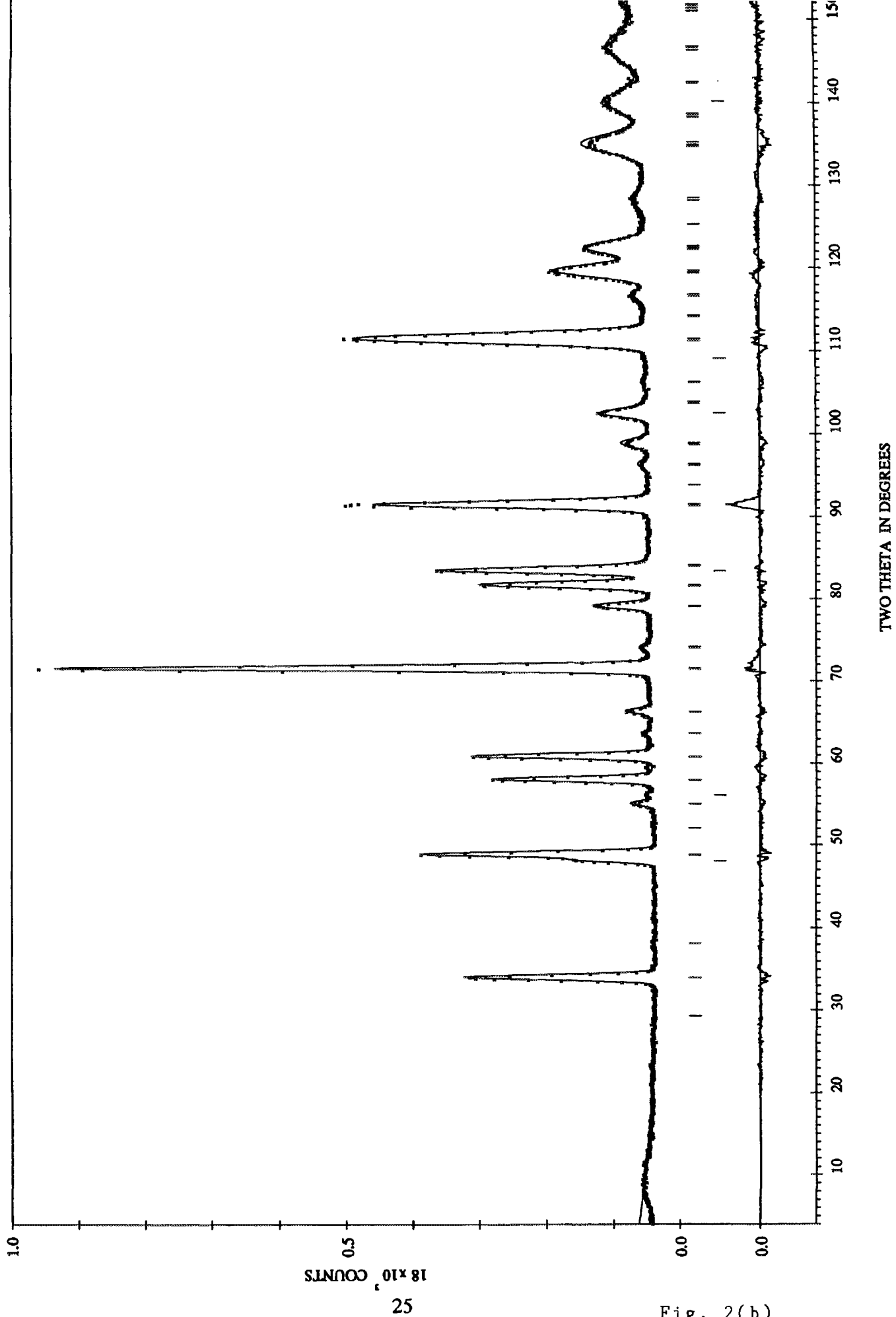


Fig. 2(b)

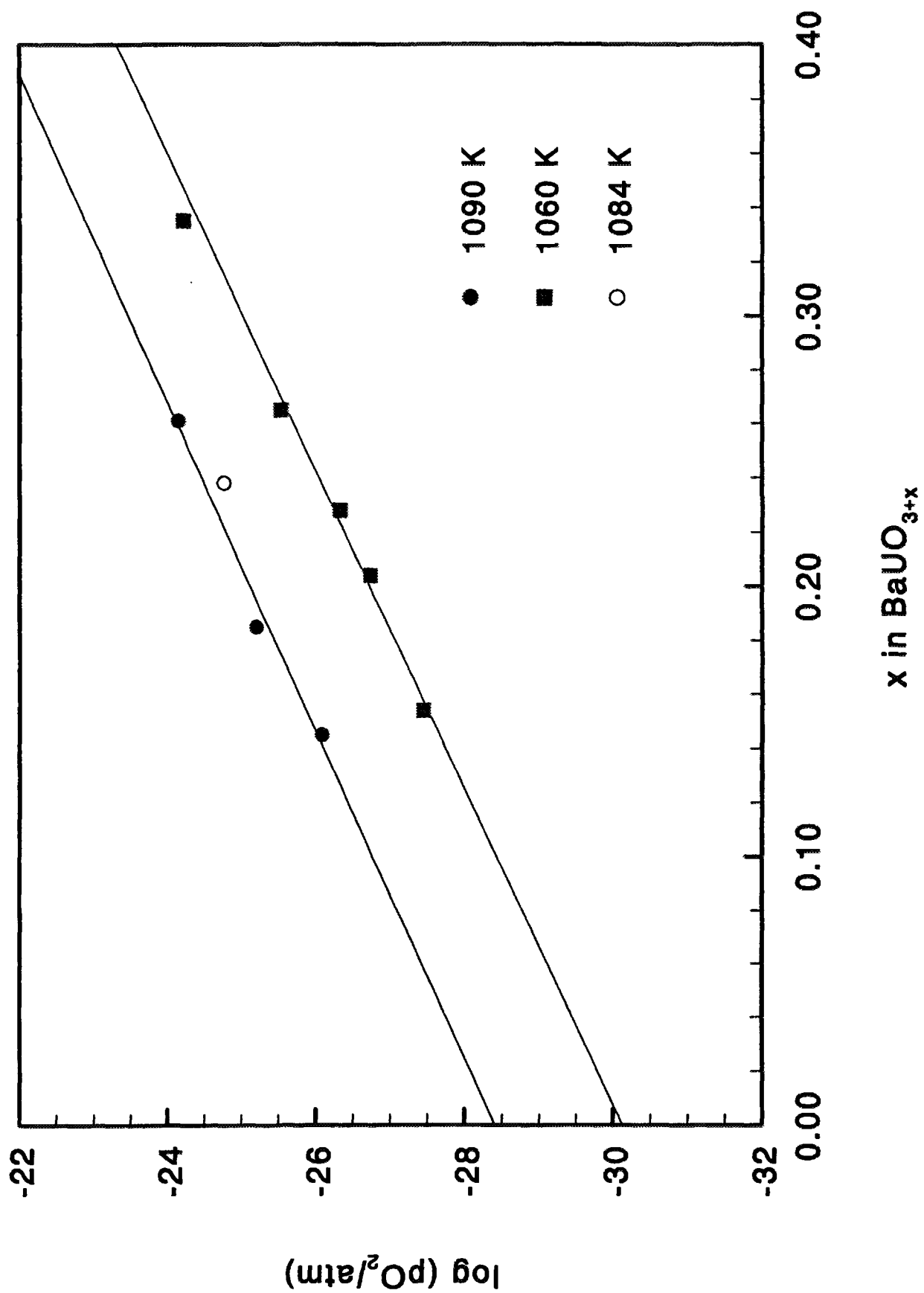


Fig. 3

